A Molecular Theory for Doubly Resonant IR−UV-vis Sum-Frequency Generation[†]

M. Hayashi,[‡] S. H. Lin,*,[§] M. B. Raschke,[‖] and Y. R. Shen[‖]

Center for Condensed Matter Sciences, National Taiwan University, 1 Roosevelt Rd., Sec. 4,
Taipei, Taiwan, 10617, ROC, Institute of Atomic and Molecular Sciences, Academia Sinica, P.O. Box 23-166,
Taipei, Taiwan 106 ROC, and Department of Physics, University of California Material Sciences Division,
Lawrence Berkeley National Laboratory, Berkeley, California 94720

The experiment for measuring doubly resonant infrared-visible (IR-vis) sum-frequency generation (SFG) has recently been developed by Shen and his co-worker and applied to Rhodamine 6G on silica surfaces. In this paper, based on the Born−Oppenheimer adiabatic approximation, a molecular theory for doubly resonant IR-vis SFG generation as a two-dimensional surface spectroscopy is presented. We shall show that this new nonlinear spectroscopy is closely related to IR and resonance Raman spectroscopy. In this preliminary theoretical derivation, the displaced harmonic potential energy surfaces model for the electronic ground and electronically excited states of the system are used to obtain the band shape functions for doubly resonant IR-vis SFG at a finite temperature. One of the unique and powerful abilities of this spectroscopy is that interference effects among IR-active modes can be observed. The calculated excitation profiles and IR spectra of the doubly resonant IR−UV SFG from Rhodamine 6G on fused silica are demonstrated. We shall show that this new nonlinear spectroscopy can provide experimentalists with access to microscopic properties of molecules on surfaces or at interfaces.

1. Introduction

Optical signal for second-order nonlinear generation is dipole-forbidden in media with inversion symmetry. However, such signals have been generated at the interfaces of isotropic media since the early days of nonlinear optics.[1,2] An important application of surface nonlinear optical measurements is the determination of adsorbate spectra via the resonant enhancement of the second-order nonlinear susceptibility χ^2. Early measurements exploited electronic resonance to record adsorbate electronic spectra.[3,4] Recently, the emphasis has been placed on the application of infrared (IR) + visible or UV sum-frequency generation (SFG) to obtain adsorbate vibrational spectra.[5−7] The vibrational spectra of a number of adsorbates have now been reported such as the methyl modes of alkanethiol self-assembled monolayers on gold;[6] a number of alcohols on silica;[2] Langmuir−Blodgett films on silica;[10,11] methoxy on Ni (111);[11] acetonitrile on ZrO_2,[12] etc. (see, e.g., ref 13).

As mentioned above, second-harmonic and sum-frequency generation (SHG/SFG) have recently found a wide rage of applications as probes in surface science due to their intrinsic surface and interface sensitivity and specificity.[14−16]

It is possible to have both ω_{IR} and ω_{vis} tunable in SFG for two-dimensional surface spectroscopy.[17] With ω_{IR} and ω_{vis} near surface vibrational and electronic transitions, respectively, SFG could be doubly resonantly enhanced. In this respect, it is similar to resonant Raman spectroscopy (RRS), which is known for its powerful applications in condensed matter physics, chemistry, and biology; however, SFG has the additional advantage of being surface specific and applicable to fluorescent molecules.

As in RRS, doubly resonant (DR) enhancement in SFG occurs only when the probed vibrational and electronic transitions are coupled. This allows for more selective spectroscopic information and better assignment of the vibrational modes. Moreover, the coupling strengths between electronic and vibrational transitions can be deduced. The technique could also be valuable for studies of intermolecular interactions at surfaces and interfaces. However, to extract molecular properties such as potential energy surfaces of molecules at surface, a molecular theory for doubly resonant IR−UV SFG intensity is needed for multimode systems.

It should be important to note here that molecular descriptions (or vibronic models) for RRS were developed and applied by many researchers.[18−42] In particular, the time-correlator approach to the Raman polarizability tensor was originally presented by Hizhnyakov and Tehver. Later, transform technique was developed based on the time-correlator approach for systems obeying the so-called standard assumptions (or the simplest vibronic model): (1) the adiabatic and Condon approximations, (2) a single electronic exited state, (3) the harmonic approximation for the vibrations, (4) linear electron-vibration coupling (displaced harmonic potential surface model), and (5) a constant damping in each of the vibrational levels of the electronic excited state.[19,22] Transform methods were subsequently extended by Page and co-workers to systems beyond these assumptions; for example, harmonic potential surfaces can be not only displaced but also distorted[25] and/or rotated (Duschinsky effect),[39] i.e., the normal-mode frequencies change upon electronic excitation as a result of quadratic electron-vibration coupling. Another extension was to non-Condon active modes.[39] Additional extensions of the transform technique included effects of inhomogeneous broadening,[34] nonadiabatic corrections,[31] anharmonicity,[36] and formal temperature average.[40,41] One major advantage of the transform technique allows one to calculate a RR profile of a Raman-active mode from the

---

[†] Part of the special issue "Noboru Mataga Festschrift".
* Corresponding author.
[‡] National Taiwan University.
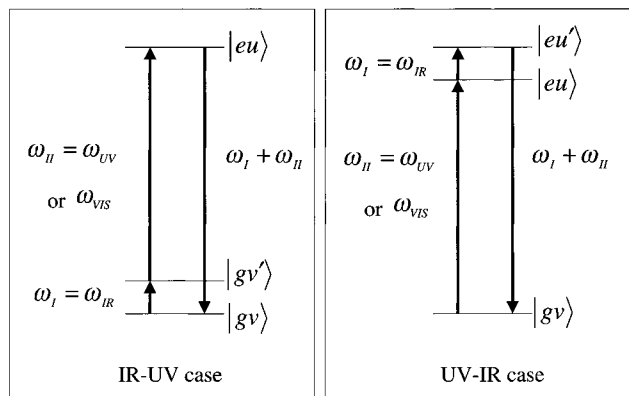[§] Academia Sinica.
[‖] University of California.

Figure 1. A schematic representation of doubly resonant IR−UV and UV−IR SFG.

measured absorption line shape using the model parameters of only this active mode while the information on the remaining inactive modes can be included via the use of the measured absorption. In this fashion, many of the complications which appear when dealing with molecular transitions within the full adiabatic approximation can be bypassed.[28]

Recent development of ab initio molecular orbital calculation methods has made it possible to provide potential surface properties of various molecules at a specific calculation level. Thus, information about part of inactive mode space can be made available, especially for high-frequency intramolecular modes. This allows one to extract "pure" information on low-frequency modes resulting from both intramolecular modes and environmental modes, which, in turn, provide molecular dynamics and/or ab initio developers with useful information for their challenging tasks to construct these low-frequency modes theoretically. In this case, a full vibronic description of inactive modes is still meaningful.

A main purpose of this paper is to provide a theoretical treatment for SFG with the doubly resonant case, i.e., IR-vis or UV. We shall also show how to apply the Born−Oppenheimer (B−O) adiabatic approximation to obtain the expressions for the doubly resonant SFG for molecular systems. In this case, as has been discussed above, we will apply the B−O adiabatic approximation to all the possible vibrational modes. It will be shown that the recasting method cannot be applied to obtain the general expression of IR−UV SFG susceptibility.[43] We shall also perform numerical simulation for model systems. In particular, we will focus on how potential energy surface properties affect doubly resonant IR−UV or vis SFG spectra. We will demonstrate how to theoretically construct doubly resonant IR-vis SFG spectra of Rhd6G on fused silica; we shall present the IR spectra and excitation profiles of doubly resonant IR-vis SFG signal of this system.

2. General Theory

We shall consider a model system shown in Figure 1. In Figure 1, g, m, k denote the initial, intermediate, final state manifolds, and ω_I, ω_II represent the frequencies of the two lasers used in SFG experiments.

According to the definition of the second-order SFG susceptibility $\chi^{(2)}_{\alpha\beta\gamma}(\omega_\text{I} + \omega_\text{II})$, i.e.,

$$P^{(2)}_\alpha(\omega_\text{I} + \omega_\text{II}) = \sum_\beta \sum_\gamma \chi^{(2)}_{\alpha\beta\gamma}(\omega_\text{I} + \omega_\text{II})E_{1\beta}(\omega_\text{I})E_{2\gamma}(\omega_\text{II}) \quad (1)$$

we find, for the doubly resonant case,[44−46]

$$\chi^{(2)}_{\alpha\beta\gamma}(\omega_\text{I} + \omega_\text{II}) = \frac{1}{\hbar^2}\sum_g \sum_m \sum_k \{\sigma_{gg}(T) - \sigma_{mm}(T)\} \times$$

$$\frac{\mu_{gk}(\alpha)\mu_{mg}(\beta)\mu_{km}(\gamma)}{[(\omega_\text{I} - \omega_{mg}) + i\Gamma_{mg}][(\omega_\text{I} + \omega_\text{II} - \omega_{kg}) + i\Gamma_{kg}]} \quad (2)$$

In eq 2, for example, $\hbar\omega_{mg} = \hbar(\omega_m - \omega_g) = E_m - E_g$, $\sigma_{gg}(T)$ is the initial population distribution function, Γ_{mg} represents the dephasing rate constant, and $\mu_{gk}(\alpha)$ denotes the α-component transition moment. In this section, we shall derive theoretical expressions for second-order susceptibility of IR−UV(vis) and UV(vis)-IR SFG in terms of a molecular description. For this purpose, we shall employ the Born−Oppenheimer adiabatic approximation and the harmonic potential surfaces for the excited and ground electronic states.

It should be noted that the term $\sigma_{mm}(T)$ in eq 2 is often ignored for the case of doubly resonant excitations and recast the dummy indices, for example, g, and m to m and g in eq 2. For the IR−UV(vis) SFG in a molecular description, $\sigma_{mm}(T)$ cannot be ignored. Herein, for simplicity we will omit notation of (vis), that is, simply using IR−UV SFG.

2.1. IR−UV SFG. In the adiabatic approximation, IR−UV SFG can be described by noting $g \rightarrow g\{v\}$, $m \rightarrow g\{v'\}$, $k \rightarrow e\{u\}$ in eq 2, where g and e denote the electronic states while $\{v\}$ and $\{u\}$ represent the vibrational states. Figure 1 shows a schematic representation of IR−UV and UV−IR SFG. For the IR−UV case, setting $\omega_\text{I} = \omega_\text{IR}$ and $\omega_\text{II} = \omega_\text{UV}$, we find

$$\chi^{(2)(\text{IR}-\text{UV})}_{\alpha\beta\gamma}(\omega_\text{IR} + \omega_\text{UV}) = \frac{1}{\hbar^2}\sum_{\{v\}} \sum_{\{v'\}} \{\sigma_{gv,gv}(T) - \sigma_{gv',gv'}(T)\} \times$$

$$\frac{\mu_{gv',gv}(\beta)}{[(\omega_\text{IR} - \omega_{gv',gv}) + i\Gamma_{gv',gv}]} \times$$

$$\sum_{\{u\}} \frac{\mu_{gv,eu}(\alpha)\mu_{eu,gv'}(\gamma)}{[(\omega_\text{IR} + \omega_\text{UV} - \omega_{eu,gv}) + i\Gamma_{eu,gv}]} \quad (3)$$

As can be seen from eq 3, this type of SFG case is very similar to resonance Raman (RR) scattering. The square of the last term (involving the summation over $\{u\}$) in eq 3 corresponds to the band-shape function of the RR excitation profile.[47,48] Equation 3 shows that the selection rule for this IR−UV SFG is that the vibrational mode should be both IR active and the resonance Raman active. (i.e., usually totally symmetric).

Here, for example, $\mu_{gv,ku}(\alpha)$ in eq 3 can be written as

$$\mu_{gv,eu}(\alpha) = \langle\Theta_{gv}|\mu_{ge}(\alpha)|\Theta_{eu}\rangle \quad (4)$$

where Θ_{gv} and Θ_{eu} denote the vibrational wave function for the normal modes. In this case, we have

$$\Theta_{gv}(Q) = \prod_{i=1}^N \chi_{gv_i}(Q_i) \text{ and } \Theta_{eu}(Q') = \prod_{i=1}^N \chi_{eu_i}(Q'_i)$$

where, for example, $\chi_{eu_i}(Q'_i)$ is the vibrational wave function for the mode i of the electronically excited state e and it is given by

$$\chi_{eu_i}(Q'_l) = N_{u_l}H_{u_l}(\sqrt{\omega'_l/\hbar}Q'_l)e^{-\omega'_l Q'^2_l}/(2\hbar) \quad (5)$$

Here $H_{u_i}(\sqrt{\omega'_l/\hbar}Q'_l)$ represents the Hermite polynomials.

We assume that the Condon approximation[49] can be applied to eq 4. It follows that

Doubly Resonant IR−UV-vis Sum Frequency Generation

J. Phys. Chem. A, Vol. 106, No. 10, 2002 **2273**

$$\mu_{gv,eu}(\alpha) = \mu_{ge}(\alpha)\langle\Theta_{gv}|\Theta_{eu}\rangle = \mu_{ge}(\alpha)\prod_{i=1}^{N}\langle\chi_{gv_i}|\chi_{eu_i}\rangle \quad (6)$$

where $\mu_{ge}(\alpha)$ represents the electronic transition moment and $\langle\chi_{gv_i}|\chi_{eu_i}\rangle$ denotes the Franck−Condon overlap integral. The non-Condon effects can be included as in the case of resonant Raman scattering. For $\mu_{gv',gv}(\beta)$, we expand $\mu_{gg}(\beta)$ with respect to the normal coordinate Q_l (for all IR active modes) to the first order and find, for $v \neq v'$,

$$\mu_{gv',gv}(\beta) = \langle\Theta_{gv'}|\mu_{gg}(\beta)|\Theta_{gv}\rangle$$

$$= \sum_{l}^{IR-active}\left(\frac{\partial\mu_{gg}(\beta)}{\partial Q_l}\right)_0\langle\Theta_{gv'}|Q_l|\Theta_{gv}\rangle$$

$$= \sum_{l}^{IR-active}\left(\frac{\partial\mu_{gg}(\beta)}{\partial Q_l}\right)_0\langle\chi_{gv'_l}|Q_l|\chi_{gv_l}\rangle\prod_{i\neq l}^{N}\delta_{gv'_i,gv_i} \quad (7)$$

where $\delta_{gv'_i,gv_i}$ represents the Kronecker-delta function. Substituting eqs 6 and 7 into eq 3 and introducing the effective vibrational dephasing rate constant $\tilde{\Gamma}_{gl}$ for the IR active mode l of the electronic ground state g and defining $\tilde{\Gamma}_{eg}$ as the effective electronic dephasing rate constant, we find a molecular expression for the second-order susceptibility of IR−UV SFG as (for the detailed derivation, see Appendix A)

$$\chi_{\alpha\beta\gamma}^{(2)(IR-UV)}(\omega_{IR} + \omega_{UV}) = \frac{1}{\hbar^2}\sum_{l}^{IR-active}\frac{A_l D_l(\omega_{IR},\omega_{UV},T)}{[(\omega_{IR} - \omega_l) + i\tilde{\Gamma}_{gl}]} \quad (8A)$$

where

$$A_l = \mu_{ge}(\alpha)\mu_{eg}(\gamma)\left(\frac{\partial\mu_{gg}(\beta)}{\partial Q_l}\right)_0$$

and

$$D_l(\omega_{IR},\omega_{UV},T) =$$
$$\sum_{\{v\}\{v'\}\{u\}}\Delta\sigma_{gv,gv'}\frac{\langle\Theta_{gv'}|Q_l|\Theta_{gv}\rangle\langle\Theta_{gv}|\Theta_{eu}\rangle\langle\Theta_{eu}|\Theta_{gv'}\rangle}{(\omega_{IR} + \omega_{UV} - \omega_{eu,gv}) + i\tilde{\Gamma}_{eg}} \quad (8B)$$

Here $\Delta\sigma_{gv,gv'} = \sigma_{gv,gv} - \sigma_{gv',gv'}$. From eq 8A, we can see that to calculate $\chi_{\alpha\beta\gamma}^{(2)(IR-UV)}(\omega_{IR} + \omega_{UV})$ it is essential to evaluate $D_l(\omega_{IR},\omega_{UV},T)$, which involves two potential surfaces, i.e., the potential surfaces of the ground electronic state and excited electronic state. It is commonly assumed that these two surfaces are harmonic. In this case, these two surfaces may be displaced but not distorted, or distorted but not displaced, or both displaced and distorted; these two surfaces may even be rotated and displaced (Duschinsky effect). In this preliminary work, we shall consider only the case in which the two surfaces are only displaced but not distorted or rotated. For the displaced oscillator case, $D_l(\omega_{IR},\omega_{UV},T)$ in eq 8A or eq 8B can be expressed as (Appendix A)

$$D_l(\omega_{IR},\omega_{UV},T) = \frac{1}{i}\int_0^\infty dt \exp[-t\{i(\omega_{eg} - \omega_{IR} - \omega_{UV}) +$$
$$\tilde{\Gamma}_{eg}\}]G_l^{IR-UV}(t,T) \quad (9)$$

where

$$G_l^{IR-UV}(t,T) = g_l^{IR-UV}(t,T)\prod_{j\neq l}^{N}g_j^{IR-UV}(t,T) \quad (10)$$

$$g_l^{IR-UV}(t,T) = \frac{-d_l}{2}(1 - e^{-it\omega_l})\exp[-S_l\{(1 + 2n_l) - n_le^{it\omega_l} -$$
$$(1 + n_l)e^{-it\omega_l}\}] \quad (11)$$

and

$$g_j^{IR-UV}(t,T) = \exp[-S_j\{(1 + 2n_j) - n_je^{it\omega_j} - (1 + n_j)e^{-it\omega_j}\}] \quad (12)$$

Note that $S_l(= \omega_l d_l^2/2\hbar)$ is the coupling constant (or Huang−Rhys factor), and $n = 1/(e^{\hbar\omega/k_BT} - 1)$.

2.2. UV−IR SFG. In a similar manner, an expression for UV−IR SFG can be derived. Using the adiabatic approximation $g \rightarrow gv$, $m \rightarrow eu$, $k \rightarrow eu'$ and noticing that $\sigma_{eu,eu}(T) \cong 0$, we obtain

$$\chi_{\alpha\beta\gamma}^{(2)(UV-IR)}(\omega_{IR} + \omega_{UV}) = \frac{1}{\hbar^2}\sum_{v}\sum_{u}\sum_{u'}\sigma_{gv,gv}(T) \times$$

$$\frac{\mu_{gv,eu}(\alpha)\mu_{eu,gv}(\beta)\mu_{eu',eu}(\gamma)}{[(\omega_{UV} - \omega_{eu,gv}) + i\Gamma_{eu,gv}][(\omega_{IR} + \omega_{UV} - \omega_{eu',gv}) + i\Gamma_{eu',gv}]} \quad (13)$$

It follows that (see Appendix B for the detailed derivation)

$$\chi_{\alpha\beta\gamma}^{(2)(UV-IR)}(\omega_{IR} + \omega_{UV}) = \frac{1}{\hbar^2}\sum_{l}^{IR-active}B_l F_l(\omega_{IR},\omega_{UV},T) \quad (14)$$

where $B_l = \mu_{ge}(\alpha)\mu_{eg}(\beta)(\partial\mu_{ee}(\gamma)/\partial Q_l)_0$ and $F_l(\omega_{IR},\omega_{UV},T)$ are given by

$$F_l(\omega_{IR},\omega_{UV},T) = \sum_{\{v\}}\sum_{\{u\}}\sum_{\{u'\}}\sigma_{gv,gv} \times$$

$$\frac{\langle\Theta_{gv}|\Theta_{eu'}\rangle\langle\Theta_{eu'}|Q_l|\Theta_{eu}\rangle\langle\Theta_{eu}|\Theta_{gv}\rangle}{[(\omega_{UV} - \omega_{eu,gv}) + i\Gamma_{eu,gv}][(\omega_{IR} + \omega_{UV} - \omega_{eu',gv}) + i\Gamma_{eu',gv}]} \quad (15A)$$

or

$$F_l(\omega_{IR},\omega_{UV},T) = \frac{1}{i}\int_0^\infty dt_1\exp[-t_1\{i(\omega_{eg} - \omega_{UV}) + \tilde{\Gamma}_{eg}\}] \times$$
$$\frac{1}{i}\int_0^\infty dt_2\exp[-t_2\{i(\omega_{eg} - \omega_{IR} - \omega_{UV}) +$$
$$\tilde{\Gamma}_{eg} + \tilde{\Gamma}_{el}\}]G_l^{UV-IR}(t_1,t_2,T) \quad (15B)$$

and $\tilde{\Gamma}_{el}$ denotes the effective vibrational dephasing rate constant for the IR active mode l of the electronically excited state e. Here $G_l^{UV-IR}(t_1,t_2,T)$ in eq 15B is given by

$$G_l^{UV-IR}(t_1,t_2,T) = g_l^{UV-IR}(t_1,t_2,T)\prod_{j\neq l}^{N}g_j^{UV-IR}(t_1,t_2,T) \quad (16)$$

where $g_j^{UV-IR}(t_1,t_2,T)$ and $g_l^{UV-IR}(t_1,t_2,T)$ are given by

$$g_j^{UV-IR}(t_1,t_2,T) = \exp[-S_j\{(1 + 2n_j) - n_je^{i(t_1+t_2)\omega_j} -$$
$$(1 + n_j)e^{-i(t_1+t_2)\omega_j}\}] \quad (17)$$

and

$$g_l^{\text{UV}-\text{IR}}(t_1,t_2,T) = \frac{d_l}{2}\{1 + n_l(1 - e^{i(t_1+t_2)\omega_l})\}e^{-it_2\omega_l} \times$$

$$\exp[-S_l\{(2n_l + 1) - (1 + n_l)e^{-i(t_1+t_2)\omega_l} - n_l e^{i(t_1+t_2)\omega_l}\}] \quad (18)$$

2.3. Inhomogeneity Effect. For the case in which the electronic transition energy is inhomogeneously distributed over the systems at various positions, the average over such inhomogeneity should be taken. We assume that the distribution function is given by a Gaussian form with the average value $\bar{\omega}_{eg}$ and its deviation δ. In this case, taking average over ω_{eg} in eq 8A with the Gaussian distribution function yields

$$\langle\chi_{\alpha\beta\gamma}^{(2)(\text{IR}-\text{UV})}(\omega_{\text{IR}} + \omega_{\text{UV}})\rangle = \frac{1}{\hbar^2}\sum_l^{\text{IR-active}}\frac{A_l\langle D_l(\omega_{\text{IR}},\omega_{\text{UV}},T)\rangle}{[(\omega_{\text{IR}} - \omega_l) + i\tilde{\Gamma}_{gl}]} \quad (19)$$

where

$$\langle D_l(\omega_{\text{IR}},\omega_{\text{UV}},T)\rangle = \frac{1}{i}\int_0^\infty dt \exp\left[-\frac{(t\delta)^2}{4} - t\{i(\bar{\omega}_{eg} - \omega_{\text{IR}} - \omega_{\text{UV}}) + \tilde{\Gamma}_{eg}\}\right]G_l^{\text{IR}-\text{UV}}(t,T) \quad (20)$$

For the UV−IR case, we notice from eq 14 that

$$\langle\chi_{\alpha\beta\gamma}^{(2)(\text{UV}-\text{IR})}(\omega_{\text{IR}} + \omega_{\text{UV}})\rangle = \frac{1}{\hbar^2}\sum_l^{\text{IR-active}} B_l\langle F_l(\omega_{\text{IR}},\omega_{\text{UV}},T)\rangle \quad (21)$$

where

$$\langle F_l(\omega_{\text{IR}},\omega_{\text{UV}},T)\rangle = \left(\frac{1}{i}\right)^2\int_0^\infty dt_1\int_0^\infty dt_2 \exp\left[-\frac{\{(t_1 + t_2)\delta\}^2}{4}\right]$$

$$\exp[-t_1\{i(\bar{\omega}_{eg} - \omega_{\text{UV}}) + \tilde{\Gamma}_{eg}\}]\exp[-t_2\{i(\bar{\omega}_{eg} - \omega_{\text{IR}} - \omega_{\text{UV}}) + \tilde{\Gamma}_{eg} + \tilde{\Gamma}_{el}\}]G_l^{\text{UV}-\text{IR}}(t_1,t_2,T) \quad (22)$$

2.4. High-Temperature Limit for Low-Frequency Modes of IR Nonactive Modes. For the case in which $\hbar\omega_l \gg k_\text{B}T$, $\hbar\omega_j \gg k_\text{B}T$ and $\hbar\omega_i < k_\text{B}T$, $G_l^{\text{IR}-\text{UV}}(t,T)$ in eq 10 becomes

$$G_l^{\text{IR}-\text{UV}}(t,T) = \bar{G}_l^{\text{IR}-\text{UV}}(t,T=0)\prod_{i\neq l}^{N_{\text{low}}}g_i^{\text{IR}-\text{UV}}(t,T) \quad (23)$$

where

$$\bar{G}_l^{\text{IR}-\text{UV}}(t,T=0) = g_l^{\text{IR}-\text{UV}}(t,T=0)\prod_{j\neq l}^{N_{\text{high}}}g_j^{\text{IR}-\text{UV}}(t,T=0) =$$

$$\frac{-d_l}{2}(1 - e^{-it\omega_l})\exp[-S_l(1 - e^{-it\omega_l})] \times$$

$$\exp[-\sum_{j\neq l}^{N_{\text{high}}}S_j(1 - e^{-it\omega_j})] \quad (24)$$

Applying the short time approximation to $g_i^{\text{IR}-\text{UV}}(t,T)$ in eq 23 leads to

$$\prod_{i\neq l}^{N_{\text{low}}}g_i^{\text{IR}-\text{UV}}(t,T) = \exp\left[-it\lambda_l' - \frac{\{t\delta_l'(T)\}^2}{4}\right] \quad (25)$$

where

$$\lambda_l' = \sum_{i\neq l}^{N_{\text{low}}}S_i\omega_i \quad (26)$$

and

$$\{\delta_l'(T)\}^2 = \sum_{i\neq l}^{N_{\text{low}}}2S_i(1 + 2n_i)(\omega_i)^2 \quad (27)$$

Note that the summations in eqs 26 and 27 are taken over i excluding $i = l$. It follows that

$$\langle D_l(\omega_{\text{IR}},\omega_{\text{UV}},T)\rangle = \int_0^\infty dt \exp\left[-\frac{\{t\Delta_l(T)\}^2}{4} - t\{i(\bar{\omega}_{eg} + \lambda_l - \omega_{\text{IR}} - \omega_{\text{UV}}) + \tilde{\Gamma}_{eg}\}\right]\bar{G}^{\text{IR}-\text{UV}}(t,T=0) \quad (28)$$

where

$$\Delta_l^2(T) = \delta^2 + \{\delta_l'(T)\}^2 \quad (29)$$

In similar fashion, we find

$$\langle F_l(\omega_{\text{IR}},\omega_{\text{UV}},T)\rangle = \left(\frac{1}{i}\right)^2\int_0^\infty dt_1\int_0^\infty dt_2 \times$$

$$\exp\left[-\frac{\{(t_1 + t_2)\Delta_l(T)\}^2}{4}\right]\exp[-t_1\{i(\bar{\omega}_{eg} - \omega_{\text{UV}}) + \tilde{\Gamma}_{eg}\}]\exp[-t_2\{i(\bar{\omega}_{eg} - \omega_{\text{IR}} - \omega_{\text{UV}}) + \tilde{\Gamma}_{eg} + \tilde{\Gamma}_{el}\}]G_l^{\text{UV}-\text{IR}}(t_1,t_2,T) \quad (30)$$

It should be noted here that in the displaced harmonic potential surface model and for the case in which when $\hbar\omega_l \gg k_\text{B}T$ holds, λ_l' is exactly the same as the half of the so-called Stokes shift of the absorption and florescence spectra (see Appendix C). In this case, the broadening factor $\{\delta_l'(T)\}^2$ in eq 29 is equal to

$$\{\delta_l'(T)\}^2 = \sum_i^{N_{\text{low}}}2S_i(1 + 2n_i)(\omega_i)^2 = \delta^2(T)$$

where the definition of $\delta^2(T)$ is given in Appendix C.

3. Results and Discussion

3.1. One-Mode System. To show the simplest application of our molecular description of the doubly resonant SFG, we shall first consider the single IR active mode case at $T = 0$ without inhomogeneous effect. From eqs 8A and 11 and using

$$\exp[S_l e^{-it\omega_l}] = \sum_{n=0}^\infty \frac{S_l^n e^{-itn\omega_l}}{n!}$$

we obtain, for the IR−UV case

$$\chi_{\alpha\beta\gamma}^{(2)(\text{IR}-\text{UV})}(\omega_{\text{IR}} + \omega_{\text{UV}}) = -\frac{A_l}{\hbar^2}\frac{d_l}{2}e^{-S_l}\frac{\bar{D}_l(\omega_{\text{IR}},\omega_{\text{UV}})}{[(\omega_{\text{IR}} - \omega_l) + i\tilde{\Gamma}_{gl}]} \quad (31)$$

where

Doubly Resonant IR−UV-vis Sum Frequency Generation

J. Phys. Chem. A, Vol. 106, No. 10, 2002 **2275**

$$\bar{D}_l(\omega_1,\omega_2) = \sum_{n=0}^{\infty} \frac{S_l^n}{n!} \left[\frac{1}{[(\omega_{IR} + \omega_{UV} - \omega_{eg} - n\omega_l) + i\tilde{\Gamma}_{eg}]} - \frac{1}{[\{\omega_{IR} + \omega_{UV} - \omega_{eg} - (1+n)\omega_l\} + i\tilde{\Gamma}_{eg}]} \right] \quad (32)$$

For the UV−IR case, we find

$$\chi_{\alpha\beta\gamma}^{(2)(UV-IR)}(\omega_{IR} + \omega_{UV}) = \frac{B_l}{\hbar^2}\frac{d_l}{2}e^{-S_l}\bar{F}_l(\omega_{IR},\omega_{UV}) \quad (33)$$

where

$$\bar{F}_l(\omega_{IR},\omega_{UV}) = \sum_{n=0}^{\infty} \frac{S_l^n}{n!} \frac{1}{[(\omega_{UV} - \omega_{eg} - n\omega_l) + i\tilde{\Gamma}_{eg}]} \times \frac{1}{[\{\omega_{IR} + \omega_{UV} - \omega_{eg} - (1+n)\omega_l\} + i(\tilde{\Gamma}_{eg} + \tilde{\Gamma}_{el})]} \quad (34)$$

3.2. Multimode System. To see the interference effect of the multi IR active mode, we shall consider a model system consisting of several IR active modes and several IR inactive modes (the number of the total modes is N) at $T = 0$ without inhomogeneous effect. In this case, we obtain

$$\chi_{\alpha\beta\gamma}^{(2)(IR-UV)}(\omega_{IR} + \omega_{UV}) = \\ -\sum_l^{IR-active} \frac{A_l}{\hbar^2}\frac{d_l}{2}e^{-S} \frac{\bar{D}_l(\omega_{IR},\omega_{UV})}{[(\omega_{IR} - \omega_l) + i\tilde{\Gamma}_{gl}]} \quad (35)$$

where $S = \sum_{i=1}^{N} S_i$ and, for example,

$$\bar{D}_l(\omega_{IR},\omega_{UV}) = \left(\prod_{i=1}^{N} \sum_{n_i=0}^{\infty} \frac{S_i^{n_i}}{n_i!} \right) \times \\ \left[\frac{1}{[(\omega_{IR} + \omega_{UV} - \omega_{eg} - n_l\omega_l - \sum_{i\neq l}^{N} n_i\omega_i) + i\tilde{\Gamma}_{eg}]} - \frac{1}{[(\omega_{IR} + \omega_{UV} - \omega_{eg} - (1+n_l)\omega_l - \sum_{i\neq l}^{N} n_i\omega_i) + i\tilde{\Gamma}_{eg}]} \right] \quad (36)$$

From eqs 35 it is obvious for multi-IR active mode systems due to the summation over l, $\chi_{\alpha\beta\gamma}^{(2)}$ depends on the sign of $A_l d_l$ of each IR active mode. This is important when the contributions of these vibrational modes overlap.

For the UV−IR case, we find

$$\chi_{\alpha\beta\gamma}^{(2)(UV-IR)}(\omega_{IR} + \omega_{UV}) = \sum_l^{IR-active} \frac{B_l}{\hbar^2}\frac{d_l}{2}e^{-S}\bar{F}_l(\omega_{IR},\omega_{UV}) \quad (37)$$

where

$$\bar{F}_l(\omega_{IR},\omega_{UV}) = \left(\prod_{i}^{N} \sum_{n_i=0}^{\infty} \frac{S_i^{n_i}}{n_i!} \right) \times \\ \left[\frac{1}{[(\omega_{UV} - \omega_{eg} - n_l\omega_l - \sum_{i\neq l}^{N} n_i\omega_i) + i\tilde{\Gamma}_{eg}]} - \frac{1}{[\{\omega_{IR} + \omega_{UV} - \omega_{eg} + (1+n_l)\omega_l + \sum_{i\neq l}^{N} n_i\omega_i\} + i(\tilde{\Gamma}_{eg} + \tilde{\Gamma}_{el})]} \right] \quad (38)$$

It is obvious from eqs 35 and 37 that the contribution of UV−IR SFG to the observed SFG signal is much smaller than that of IR−UV SFG (the ratio is approximately given by $\tilde{\Gamma}_{gl}/\tilde{\Gamma}_{eg}$).

We have so far considered the doubly resonance case only. Order estimations of ratios of the nonresonance cases to the IR−UV doubly resonance case are considered in Appendix D. For example, we find that for two mixed resonant/nonresonant cases their intensity ratios can be approximately given by $\tilde{\Gamma}_{gl}/\omega_{II}$ and $\tilde{\Gamma}_{gl}/\omega_I$; thus even for these two cases, the contributions can be ignored when comparing them with the doubly resonant case.

3.3. Numerical Simulation. *3.3.1. Model Systems.* To understand some of the basic properties of doubly resonant IR-vis SFG spectra, we shall discuss a model system consisting of a single IR mode. In this case, we can use eqs 31 and 33 for simulation. In this paper, for example, circular frequency [ω] $= s^{-1}$ can be transformed into wavenumber units as [$\omega/2\pi c$] $=$ cm^{-1} where c denotes the velocity of light. Hereafter, we simply denote ω_i, $\tilde{\Gamma}_i$, Δ_i, etc. as parameters thus-transformed into wavenumber units. We now choose parameters as follows; $\omega_{eg} = 18500$ cm^{-1}, $\tilde{\Gamma}_{eg} = 100$ cm^{-1}, $\omega_l = 1654$ cm^{-1}, $\tilde{\Gamma}_{gl} = \tilde{\Gamma}_{el} = 8$ cm^{-1}.

Figure 2 shows doubly resonant IR-vis SFG spectra as a function of the wavelength of the visible laser and the wavenumber of the IR laser. In Figure 2, three-dimension spectra of the model system are shown with several Huang−Rhys factors, i.e., $S = 0.01, 0.1, 0.2, 0.5,$ and 1.0. Equation 31 implies that if the broadening effect is very small, two peaks will appear in the excitation profiles for the case in which the S values are less than 0.1. This implies that even in such a small coupling case, the excitation profile of IR-vis SFG becomes broader than the absorption spectrum.

Figure 2 also shows that when the S values are larger than 0.2, the SFG spectra exhibit multiple peaks toward the shorter wavelength region of the λ_{vis} axis. It should be noted here that in the case of $S = 1.0$, only three peaks can be seen instead of four peaks as shown in the $S = 0.5$ case. This is simply due to the fact that for $S = 1.0$, the Franck−Condon overlap integral contributions of the transition of $v = 0$ to $u = 1$ and the transition $v = 0$ and $u = 0$ cancel each other (see eq 32).

To see more details of the λ_{vis} dependence, Figure 3 presents the calculated excitation profiles of IR-vis SFG at $\omega_{IR} = \omega_l$. Figure 3 clearly shows that if the S values are less than 0.1, the intensity of the second peak at the shorter wavelength becomes larger than that at the 0−0 transition.

The calculated IR spectra of SFG at $\omega_{vis} = \omega_{eg}$ are shown in Figure 4. Notably, the IR intensity with $S = 0.2$ is almost the same as that with $S = 1.0$. This is due to the rather exceptional behavior of the Franck−Condon overlap integral with $S = 1.0$.
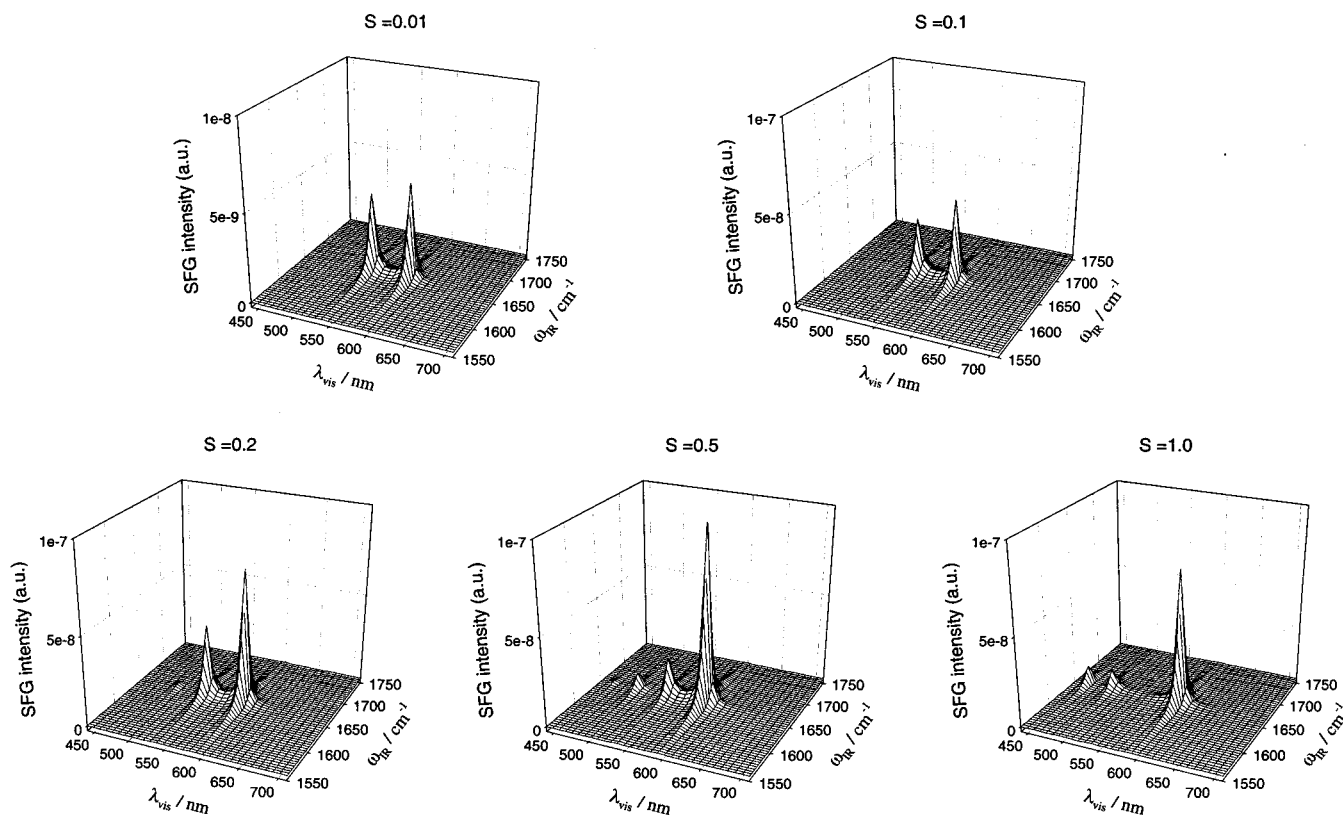
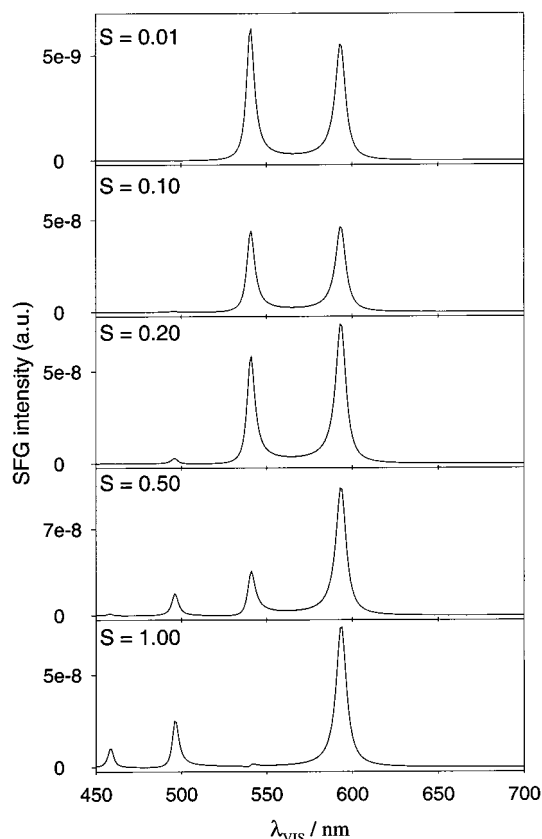**Figure 2.** The calculated three-dimensional spectra of IR−UV SFG for a single IR-active mode system.

Figure 3. The calculated excitation profiles of SFG intensity at $\omega_{IR} = \omega_l$. The calculation is performed for the model used in Figure 2.

Let us next consider a model system comprising four IR-active modes. In this case, as mentioned in the previous section, the sign of $A_l \times d_l$ in eq 35 should lead to important effects on
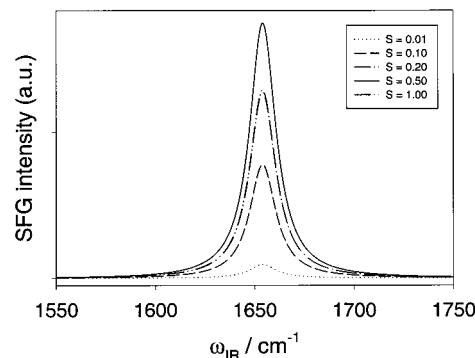

Figure 4. The calculated IR spectra of SFG intensity at $\omega_{\text{vis}} = \omega_{eg}$. The calculation is performed for the model used in Figure 2.

IR-vis SFG spectra. We set the vibrational frequencies; $\omega_1 = 1514$ cm^{-1}, $\omega_2 = 1575$ cm^{-1}, $\omega_3 = 1617$ cm^{-1}, $\omega_4 = 1654$ cm^{-1}, the vibrational dephasing rate constants $\tilde{\Gamma}_{g1} = \tilde{\Gamma}_{g2} = \tilde{\Gamma}_{g3} = 8.0$ cm^{-1} and $\tilde{\Gamma}_{g4} = 10.0$ cm^{-1}, and the Huang−Rhys factors $S_1 = 0.0018$, $S_2 = 0.01$, $S_3 = 0.00035$, and $S_4 = 0.05$. The remaining parameters are the same as those used in Figure 2.

We now refer, for example, mppp as a set of the signs of $\{A_l \times d_l\}$ for the four modes

$$\{\text{sign}(A_1d_1) = -, \text{sign}(A_2d_2) = +, \text{sign}(A_3d_3) = +, \text{sign}(A_4d_4) = +\}$$

Here, for simplicity, we fix the values of $|A_l|$ as 4.5, 0.8, 7.5, 1.5 (for $l = 1, 2, 3, 4$). We first consider only one mode having a different sign. In this case, we have four cases, i.e., mppp, pmpp, ppmp, and pppm. Figure 5a presents the calculated results. One can see that two IR peaks can be significantly overlapped. The arrows indicate the most obvious interference effects. Since the IR peaks at $\omega_1 = 1514$ cm^{-1} and $\omega_2 = 1575$

Doubly Resonant IR−UV-vis Sum Frequency Generation

J. Phys. Chem. A, Vol. 106, No. 10, 2002 **2277**
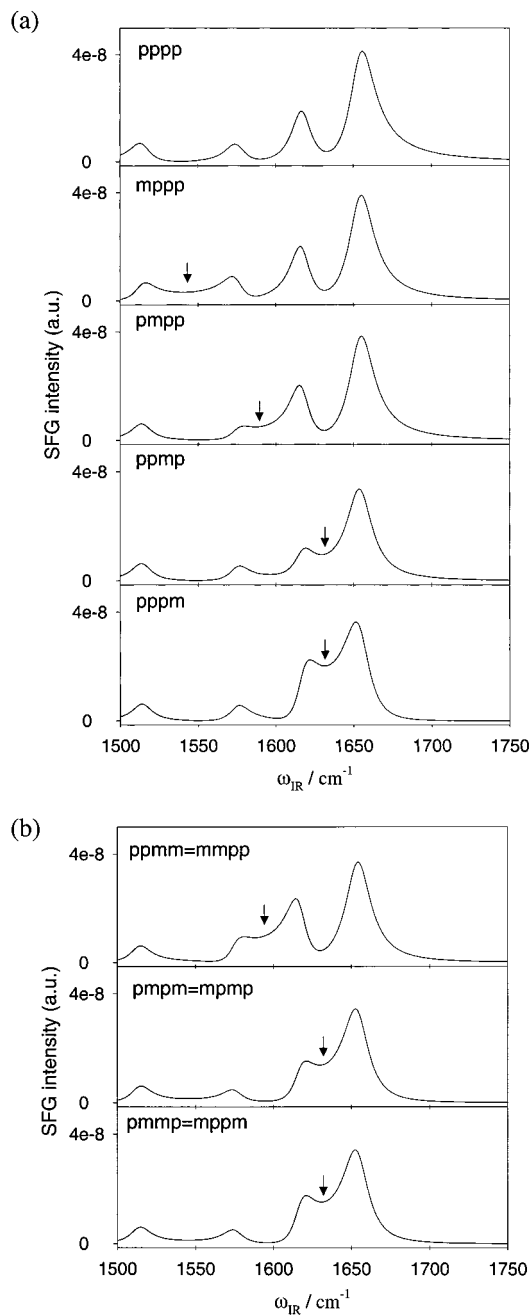
(a)

(b)

Figure 5. The calculated interference effects of IR spectra of SFG intensity for a four-IR active mode system. The calculations are carried out for (a) one of the four signs is different, and (b) two of the four are different.

cm^{-1} are the most separated from the next neighbor ones, we cannot see any significant interference effects in the mppp case. One can also consider the case in which two of the four signs are the same. In this case, six cases can be investigated. The calculated results are shown in Figure 5b. From this calculation, we find that only three possibilities are relevant in this case. The most obvious interference effect is again shown by the arrow in each panel.

3.3.2. Rhodamine 6G. We are now in a position to apply the formulas presented in section 3 to investigate IR-vis doubly resonant SFG spectra of Rhodamine 6G (Rhd6G) adsorbed on fused silica. This system has been well studied in the past.[3,50−52] For the purpose of illustration, IR-vis doubly resonant SFG spectra will be calculated in this paper. Notice that for this

system, we shall use the same parameters as those used in Figure 4 plus the following additional one IR inactive mode: $\omega_{in} = 1300\ cm^{-1}$, $\tilde{\Gamma}_{in} = 8.0\ cm^{-1}$, $S_{in} = 0.1106$. Here the ω_{in} mode is adopted from a previous study of Rhd6G.[44] We also set effective inhomogeneity as $\Delta_l(T) = \sqrt{\delta^2 + \{\delta_l(T)\}^2} = 800\ cm^{-1}$ for the four modes. These values, the ones for the four IR active modes, and $\bar{\omega}_{eg}$ are determined so that the calculated absorption spectrum, the calculated SFG excitation profiles, and the calculated SFG IR spectra can best capture the characteristics of the observed ones. It should be noted that these values may be altered depending on more precise experimental observation or more data at various λ_{vis} and ω_{IR}. The relative values of A_l can be deduced from an IR absorption measurement of Rh6G dissolved in solid KBr. The deduced values are $|A_1| = 4.5$, $|A_2| = 0.8$, $|A_3| = 7.5$, and $|A_4| = 1.5$.

In Figure 6a, the SFG signals at $\lambda_{vis} = 495$, 532, and 586 nm are calculated as a function of ω_{IR}. For comparison, we also show the observed spectra in the right-hand side of Figure 6a. For the observed spectra, as the wavelength of the visible laser becomes longer, the intensity of the SFG signal increases. A similar feature can be seen in the calculated spectra. We also simulate the excitation profiles of the SFG signal. The results are shown in Figure 6b. For reference, the observed excitation profiles are also shown in the lower panel of Figure 6b. In both panels, the solid lines denote the corresponding absorption spectrum. From Figure 6b, a similar IR wavenumber dependence can be seen in both the calculated and observed excitation profiles. It is important to note that inclusion of the $\omega_{in} = 1300\ cm^{-1}$ mode is very important to reproduce characteristics of the observed absorption spectra in the shorter wavelength region.

4. Conclusion

We have presented a molecular description of IR−UV and UV−IR SFG signals based on the use of the adiabatic approximation. In this preliminary study, we have used the displaced harmonic potential energy surfaces model for the electronic ground and electronically excited states of the system. By applying the Slater sum and the contour integral, we have obtained the nuclear correlation functions for both IR-active and inactive modes at a finite temperature. We have found that the so-called recasting method cannot be applied to a molecular system at a finite temperature. The final form of the resulting expression has been presented in terms of the summation over IR-active modes. In this representation, it is obvious that for the case in which a molecular system consists of several IR-active modes, the interference effects among these modes should be taken into account. Our theoretical expression of IR−UV SFG implies that given a precise value (including its sign) of the first derivative of the permanent dipole moment of the IR-active mode, the relative direction of the displacement of the potential energy surfaces can be determined or vice-versa. Therefore, doubly resonant IR−UV SFG has a powerful ability to determine microscopic properties of molecules on surfaces or at interfaces.

As an application, we have shown how to reconstruct the excitation profiles and IR spectra of the doubly resonant IR−UV SFG for Rhd6G on fused silica. Using the determined physical parameters, we can reproduce the characteristics of the observed SFG results and absorption spectra. We can also construct fluorescence spectra.

In summary, in this paper, we have shown that the new doubly resonant IR-vis SFG is closely related to IR spectra and resonance Raman (RR) spectra in the sense that the active vibrational modes in this new nonlinear spectroscopy should
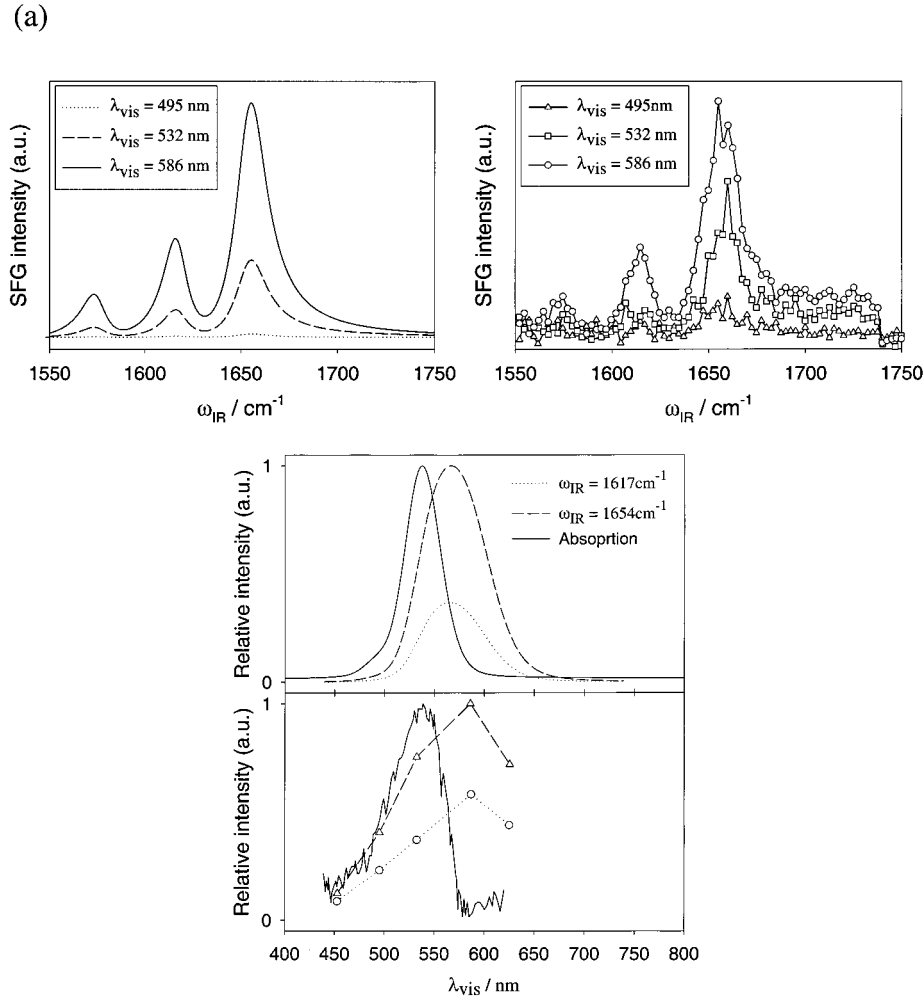
(a)

Figure 6. The calculated SFG intensity of Rhd6G. The calculations are performed for (a) IR spectra and (b) excitation profiles. The observed data are shown in each panel. The calculated and observed absorption spectra are also superimposed in panel (b).

be both IR active and RR active. A distinct advantage of this nonlinear spectroscopy is that unlike RRS, it can be applied to fluorescent molecules, so one can expect that it will soon become a very powerful spectroscopy.

Appendix A. Detailed Derivation of Equation 8A

We recall that

$$\sigma_{gv,gv}(T) = \sigma_{gv_l}(T)\prod_{j\neq l}^{N}\sigma_{gv_j}(T)$$

where, for example,

$$\sigma_{gv_l}(T) = \frac{e^{-(v_l+1/2)\hbar\omega_l/k_B T}}{\sum_{v_l}^{\infty}e^{-(v_l+1/2)\hbar\omega_l/k_B T}}$$

It follows that

$$\sigma_{gv,gv}(T) - \sigma_{gv',gv'}(T) = \sigma_{gv_l}(T)(\prod_{j\neq l}^{N}\sigma_{gv_j}(T))[1 -$$

$$e^{-(v'_l-v_l)\hbar\omega_l/k_B T}(\prod_{j\neq l}^{N}e^{-(v'_j-v_j)\hbar\omega_j/k_B T})] \quad (A1)$$

From eq 3, we find

$$\chi_{\alpha\beta\gamma}^{(2)(\text{IR-UV})}(\omega_{\text{IR}}+\omega_{\text{UV}}) = \frac{1}{\hbar^2}\sum_l A_l \sum_{v_l}\sum_{v'_l}\sum_{u_l}(\prod_{j\neq l}^{N}\sum_{v_j}\sum_{v'_j}\sum_{u_j}) \times$$

$$[1 - e^{-(v'_l-v_l)\hbar\omega_l/k_B T}(\prod_{j\neq l}^{N}e^{-(v'_j-v_j)\hbar\omega_j/k_B T})] \times$$

$$\frac{\sigma_{gv_l}(T)\langle\chi_{gv'_l}|Q_l|\chi_{gv_l}\rangle\langle\chi_{gv_l}|\chi_{eu_l}\rangle\langle\chi_{eu_l}|\chi_{gv'_l}\rangle}{\{\omega_{\text{IR}} - (v'_l - v_l) - \sum_{j\neq l}^{N}(v'_j - v_j)\} + i\Gamma_{gv'_1\cdots v'_l\cdots v'_N, gv'_1\cdots v'_l\cdots v_N}} \times$$

$$\frac{(\prod_{j\neq l}^{N}\sigma_{gv_j}(T)\langle\chi_{gv_j}|\chi_{ku_j}\rangle\langle\chi_{ku_j}|\chi_{gv'_j}\rangle\delta_{gv'_j,gv_j})}{\{\omega_{\text{IR}}+\omega_{\text{UV}} - \omega_{eg} - (u_l - v_l)\omega_l - \sum_{j\neq l}^{N}(u_j - v_j)\omega_j\} + i\Gamma_{eu_1\cdots u_l\cdots u_N, gv_1\cdots v_l\cdots v_N}]$$

$$(A2)$$

We shall, for simplicity, assume that the vibrational quantum number dependence of dephasing rate constants can be ignored, i.e., $\Gamma_{gv_l+1,gv_l} \approx \tilde{\Gamma}_{gl}$ and $\Gamma_{eu_1\cdots u_l\cdots u_N,gv_1\cdots v_l\cdots v_N} \approx \tilde{\Gamma}_{eg}$. In this case,

Doubly Resonant IR−UV-vis Sum Frequency Generation

J. Phys. Chem. A, Vol. 106, No. 10, 2002 **2279**

using the formula

$$\frac{1}{x} = \int_0^\infty dt\, e^{-tx}$$

we find

$$\chi^{(2)(IR-UV)}_{\alpha\beta\chi}(\omega_{IR} + \omega_{UV}) =$$

$$\frac{1}{\hbar^2} \sum_l^{IR-active} \frac{A_l}{(\omega_{IR} - \omega_l) + i\tilde{\Gamma}_{gl}} D_l(\omega_{IR},\omega_{UV},T) \quad (A3)$$

where

$$D_l(\omega_{IR},\omega_{UV},T) = \frac{1}{i}\int_0^\infty dt \exp[-t\{i\{\omega_{eg} - \omega_{IR} - \omega_{UV}\} + \tilde{\Gamma}_{eg}\}]G_l^{IR-UV}(t,T) \quad (A4a)$$

$$G_l^{IR-UV}(t,T) = g_l^{IR-UV}(t,T)\prod_{j\neq l}^N g_j^{IR-UV}(t,T) \quad (A4b)$$

$$g_l^{IR-UV}(t,T) = (1 - e^{-\hbar\omega_l/k_BT}) \times$$

$$\sum_{u_l}\sum_{v_l}\sigma_{gv_l}(T)\sqrt{\frac{(1+v_l)\hbar}{2\omega_l}}\langle\chi_{gv_l}|\chi_{eu_l}\rangle\langle\chi_{eu_l}|\chi_{gv_l+1}\rangle \times$$

$$e^{-t[i\omega_l\{(u_l+1/2)-(v_l+1/2)\}]} \quad (A4c)$$

and

$$g_j^{IR-UV}(t,T) = \sum_{v_i}\sum_{u_i}\sigma_{gv_i}(T)|\langle\chi_{gv_i}|\chi_{eu_i}\rangle|^2\, e^{-t[i\omega_l\{(u_l+1/2)-(v_l+1/2)\}]}$$

$$(A4d)$$

Since eq A4d is a well-known function, let us only consider eq A4b. Equation A4b can be rewritten as

$$g_l^{IR-UV}(t,T) =$$

$$(1 - e^{-\hbar\omega_l/k_BT})\sum_{v_l}\sigma_{gv_l}(T)e^{it\omega_l(v_l+1/2)}\frac{\sqrt{\omega_l/(\hbar\pi)}}{2^{v_l+1}v_l!}\int_{-\infty}^\infty\int_{-\infty}^\infty$$

$$dQ_l\, d\bar{Q}_l \times H_{gv_l}(\sqrt{\omega_l/\hbar}Q_l)H_{gv_{l+1}}(\sqrt{\omega_l/\hbar}\bar{Q}_l)e^{-(\omega_l/2\hbar)(Q_l^2+\bar{Q}_l^2)} \times$$

$$\sum_{u_l}\frac{e^{-it\omega_l(u_l+1/2)}}{\sqrt{\pi}2^{u_l}u_l!}H_{eu_l}(\sqrt{\omega_l/\hbar}Q_l')H_{eu_l}(\sqrt{\omega_l/\hbar}\bar{Q}_l')e^{-\omega_l/2\hbar(Q_l'^2+\bar{Q}_l'^2)}$$

$$(A5)$$

Applying the Slater sum[53] to eq A5, we obtain

$$g_l^{IR-UV}(t,T) =$$

$$(1 - e^{-\hbar\omega_l/k_BT})\sum_{v_l}\sigma_{gv_l}(T)e^{\mu_l(v_l+1/2)}\frac{\sqrt{\omega_l/(\hbar\pi)}}{2^{v_l+1}v_l!}\int_{-\infty}^\infty\int_{-\infty}^\infty$$

$$dQ_l\, d\bar{Q}_l \times H_{gv_l}(\sqrt{\omega_l/\hbar}Q_l)H_{gv_{l+1}}(\sqrt{\omega_l/\hbar}\bar{Q}_l)e^{-(\omega_l/2\hbar)(Q_l^2+\bar{Q}_l^2)} \times$$

$$\frac{1}{\sqrt{2\pi\sinh\mu_l}}\exp\left[-\frac{\omega_l}{4\hbar}\left\{(Q_l'+\bar{Q}_l')^2\tanh\frac{\mu_l}{2} + (Q_l'-\bar{Q}_l')^2\coth\frac{\mu_l}{2}\right\}\right] \quad (A6)$$

where $\mu_l = it\omega_l$. Using the complex integral form of Hermite polynomials, eq A6 can be rewritten as

$$g_l^{IR-UV}(t,T) =$$

$$(1 - e^{-\hbar\omega_l/k_BT})\sum_{v_l}\sigma_{gv_l}(T)e^{\mu_l(v_l+1/2)}\frac{\sqrt{\omega_l/(\hbar\pi)}}{2^{v_l+1}v_l!}\int_{-\infty}^\infty\int_{-\infty}^\infty \times$$

$$dQ_l\, d\bar{Q}_l \times (-1)\frac{v_l!}{2\pi i}\frac{(v_l+1)!}{2\pi i}\oint dZ_1$$

$$\oint dZ_2\frac{e^{-Z_1^2-2Z_1(\omega_l/\hbar)^{1/2}Q_l}}{Z_1^{v_l+1}}\frac{e^{-Z_2^2-2Z_2(\omega_l/\hbar)^{1/2}\bar{Q}_l}}{Z_2^{v_l+2}} \times$$

$$\exp\left[-\frac{\omega_l}{4\hbar}\{(Q_l+\bar{Q}_l)^2 + (Q_l-\bar{Q}_l)^2\}\right] \times$$

$$\frac{1}{\sqrt{2\pi\sinh\mu_l}}\exp\left[-\frac{\omega_l}{4\hbar}\left\{(Q_l'+\bar{Q}_l')^2\tanh\frac{\mu_l}{2} + \right.\right.$$

$$\left.\left.(Q_l'-\bar{Q}_l')^2\coth\frac{\mu_l}{2}\right\}\right] \quad (A7)$$

where $Q_l' = Q_l + d_l$. Noticing that $\sigma_{gv_l}(T) = (2\sinh\hbar\omega_l/2k_BT)e^{-(v_l+1/2)\hbar\omega_l/k_BT}$ and defining $x = Q_l + \bar{Q}_l$ and $y = Q_l - \bar{Q}_l$ in eq A7, we find

$$g_l^{IR-UV}(t,T) =$$

$$(1 - e^{-\hbar\omega_l/k_BT})\sum_{v_l}\sigma_{gv_l}(T)e^{\mu_l(v_l+1/2)}\frac{\sqrt{\omega_l/\hbar}}{2^{v_l+2}\pi}\frac{1}{\sqrt{2\sinh\mu_l}} \times$$

$$\frac{(-1)}{2\pi i}\frac{(v_l+1)!}{2\pi i}\oint dZ_1\oint dZ_2\frac{e^{-Z_1^2}}{Z_1^{v_l+1}}\frac{e^{-Z_2^2}}{Z_2^{v_l+2}}\exp\left[-\right.$$

$$\frac{\omega_l d^2}{\hbar}\tanh\frac{\mu_l}{2}\right]\int_{-\infty}^\infty dx\exp\left[-\frac{\omega_l}{4\hbar}\left(1+\tanh\frac{\mu_l}{2}\right)x^2 -\right.$$

$$\left.\frac{\omega_l}{4\hbar}\left(\tanh\frac{\mu_l}{2}\right)4d_lx - \sqrt{\omega_l/\hbar}(Z_1+Z_2)x\right]\int_{-\infty}^\infty dy\exp\left[-\right.$$

$$\left.\frac{\omega_l}{4\hbar}\left(1+\coth\frac{\mu_l}{2}\right)y^2 - \sqrt{\omega_l/\hbar}(Z_1-Z_2)y\right] \quad (A8)$$

Performing the integrals over x and y and then performing the complex integral over Z_2 yields

$$g_l^{IR-UV}(t,T) = \frac{(1 - e^{-\hbar\omega_l/k_BT})}{2\sqrt{\omega_l/\hbar}}\left(2\sinh\frac{\hbar\omega_l/k_BT}{2}\right)e^{-\hbar\omega_l/k_BT} \times$$

$$\sum_{v_l}\left[\frac{e^{-\hbar\omega_l/k_BT}e^{\mu_l}}{2}\right]^{v_l}\exp[-S_l(1-e^{-\mu_l})]\frac{(-1)}{2\pi i}\oint dZ_1\frac{1}{Z_1^{v_l+1}} \times$$

$$\exp[\sqrt{\omega_l/\hbar}d_l(1-e^{-\mu_l})Z_1]\,\{2e^{-\mu_l}Z_1 + \sqrt{\omega_l/\hbar}\,d_l(1-e^{-\mu_l})\}^{v_l+1} \quad (A9)$$

Using $\sum_{n=0}^\infty A^n = 1/(1-A)$ and applying the Cauchy integral theorem to eq A9 leads to

$$g_l^{\mathrm{IR-UV}}(t,T) = \frac{-d_l}{2}(1 - e^{-it\omega_l}) \exp[-S_l\{(1 + 2n_l) - $$
$$n_l e^{it\omega_l} - (1 + n_l)e^{-it\omega_l}\}] \quad \text{(A10)}$$

where $n_l = 1/(e^{\hbar\omega_l/k_B T} - 1)$.

It is important to note here that if we ignore $\sigma_{gv,gv}(T) - \sigma_{gv',gv'}(T)$ in eq A1, $g_l^{\mathrm{IR-UV}}(t,T)$ then becomes

$$g_l^{\mathrm{IR-UV}}(t,T) = \frac{-d_l}{2}(1 - e^{-it\omega_l})(1 + n_l) \exp[-S_l\{(1 + $$
$$2n_l) - n_l e^{it\omega_l} - (1 + n_l)e^{-it\omega_l}\}] \quad \text{(A11)}$$

Appendix B: Detailed Derivation of Equation 14

Equation 13 can be written in a fashion similar to that used in Appendix A as

$$\chi_{\alpha\beta\gamma}^{(2)}(\omega_{\mathrm{IR}} + \omega_{\mathrm{UV}}) = \frac{1}{\hbar^2} \sum_l^{\mathrm{IR-active}} A_l \frac{1}{i} \int_0^\infty dt_1 \exp[-t_1\{i(\omega_{eg} - $$
$$\omega_{\mathrm{UV}}) + \Gamma_{eg}\}] \frac{1}{i} \int_0^\infty dt_2 \exp[-t_2\{i(\omega_{eg} - \omega_{\mathrm{IR}} - \omega_{\mathrm{UV}}) + $$
$$\Gamma_{eg} + \Gamma_{el}\}] G_l^{\mathrm{UV-IR}}(t_1,t_2,T) \quad \text{(B1)}$$

where

$$G_l^{\mathrm{UV-IR}}(t_1,t_2,T) = g_l^{\mathrm{UV-IR}}(t_1,t_2,T) \prod_{j\neq l}^{N} g_j^{\mathrm{UV-IR}}(t_1,t_2,T) \quad \text{(B2a)}$$

$$g_l^{\mathrm{UV-IR}}(t_1,t_2,T) = $$
$$\sum_{u_l}\sum_{v_l}\sigma_{gv_l}(T)\sqrt{\frac{(u_l+1)\hbar}{2\omega_l}}\langle\chi_{gv_l}|\chi_{eu_l+1}\rangle\langle\chi_{eu_l}|\chi_{gv_l}\rangle \exp[-i(t_1 + t_2)$$
$$\{(u_l + 1/2)\omega_l - (v_l + 1/2)\omega_l\}] \exp[-it_2\omega_l] \quad \text{(B2b)}$$

and

$$g_j^{\mathrm{UV-IR}}(t_1,t_2,T) = \sum_{v_j}\sum_{u_j}\sigma_{gv_j}(T)|\langle\chi_{gv_j}|\chi_{eu_j}\rangle|^2 \times$$
$$\exp[-i(t_1 + t_2)\{(u_j + 1/2)\omega_j - (v_j + 1/2)\omega_j\}] \quad \text{(B2c)}$$

Since eq B2c is exactly the same as eq A4d if $t_1 + t_2$ is referred to t, here we consider eq B2b. Applying the Slater sum to eq B2b yields

$$g_l^{\mathrm{UV-IR}}(t_1,t_2,T) = e^{-it_2\omega_l}\left(\sinh\frac{\hbar\omega}{2kT}\right)\sum_{u_l}\frac{e^{-\mu_l(u_l+1/2)}\sqrt{\omega_l/(\hbar\pi)}}{\sqrt{2\pi\sinh\lambda_l}\ 2^{u_l}u_l!} \times$$
$$\frac{(-1)(u_l!)(u_l+1)!}{(2\pi i)^2}\oint dZ_1\frac{e^{-Z_1^2}}{Z_1^{u_l+2}}\oint dZ_2\frac{e^{-Z_2^2}}{Z_2^{u_l+1}} \times$$
$$\int_{-\infty}^{\infty}\int_{-\infty}^{\infty} dQ_l\, d\bar{Q}_l \exp\left[-\frac{\omega_l}{4\hbar}\{(Q_l' + \bar{Q}_l')^2 + (Q_l' - \bar{Q}_l')^2\}\right] \times$$
$$\exp\left[-\frac{\omega_l}{4\hbar}\left\{(Q_l + \bar{Q}_l)^2\tanh\frac{\lambda_l}{2} + (Q_l - \bar{Q}_l)^2\coth\frac{\lambda_l}{2}\right\}\right] \times$$
$$\exp[-2\sqrt{\omega_l/\hbar}Z_1 Q_l' - 2\sqrt{\omega_l/\hbar}Z_2\bar{Q}_l'] \quad \text{(B3)}$$

where $\lambda_l = \hbar\omega_l/k_B T - i(t_1 + t_2)\omega_l = \hbar\omega_l/k_B T - \mu_l$. Defining $Q_l' = Q_l + d_l$ and performing the integrals over Q_l and $\bar{Q}_l$ leads to

$$g_l^{\mathrm{UV-IR}}(t_1,t_2,T) = $$
$$e^{-it_2\omega_l-\mu_l/2}\left(\sinh\frac{\hbar\omega}{2k_B T}\right)\sqrt{\frac{1}{(\omega_l/\hbar)e^{\lambda_l}}}\sum_{u_l}\frac{e^{-\mu_l u_l}}{2^{u_l}}\exp[-S_l(1 - $$
$$e^{-\lambda_l})]\frac{(-1)}{2\pi i}\oint dZ_2\frac{1}{Z_2^{u_l+1}}\exp[-d_l\sqrt{\omega_l/\hbar}(1 - e^{-\lambda_l})Z_2] \times$$
$$\frac{(u_l + 1)!}{2\pi i}\oint dZ_1\frac{1}{Z_1^{u_l+2}}\exp[-d_l\sqrt{\omega_l/\hbar}(1 - e^{-\lambda_l})Z_1 + $$
$$2e^{-\lambda_l}Z_2 Z_1] \quad \text{(B4)}$$

Noticing that

$$\frac{(n + 1)!}{2\pi i}\oint dZ\frac{1}{Z^{n+2}}\exp[\varsigma Z_n] = \varsigma^{n+1}$$

we obtain

$$g_l^{\mathrm{UV-IR}}(t_1,t_2,T) = e^{-it_2\omega_l-(\lambda_l+\mu_l)/2}\frac{\left(\sinh\frac{\hbar\omega_l}{2kT}\right)}{\sqrt{\omega_l/\hbar}}\exp[-S_l(1 - $$
$$e^{-\lambda_l})]\frac{(-1)}{(2\pi i)}\oint dZ_2\{2e^{-\lambda_l}Z_2 - d_l\sqrt{\omega_l/\hbar}(1 - e^{-\lambda_l})\} \times$$
$$\frac{1/(1 - e^{-\lambda_l-\mu_l})}{Z_2 + \frac{d_l\sqrt{\omega_l/\hbar}(e^{-\mu_l} - e^{-\lambda_l-\mu_l})}{(2 - 2e^{-\lambda_l-\mu_l})}}\exp[-d_l\sqrt{\omega_l/\hbar}(1 - e^{-\lambda_l})Z_2]\Big\}$$
$$\text{(B5)}$$

Applying the Cauchy integral theorem to eq B5 finally yields

$$g_l^{\mathrm{UV-IR}}(t_1,t_2,T) = \frac{d_l}{2}\{1 + n_l(1 - e^{i(t_1+t_2)\omega_l})\}\,e^{-it_2\omega_l} \times$$
$$\exp[-S_l\{(2n_l + 1) - (1 + n_l)e^{-i(t_1+t_2)\omega_l} - n_l e^{i(t_1+t_2)\omega_l}\}] \quad \text{(B6)}$$

A similar method can be applied to eq B2c; we find

$$g_j^{\mathrm{UV-IR}}(t_1,t_2,T) = \exp[-S_j\{(1 + 2n_j) - n_j e^{i(t_1+t_2)\omega_j} - $$
$$(1 + n_j)e^{-i(t_1+t_2)\omega_j}\}] \quad \text{(B7)}$$

Appendix C: Absorption and Fluorescence Spectra

It should be important to show the band-shape functions of the absorption and fluorescence spectra; they are, respectively,

$$A(\omega_{\mathrm{UV}}) = 2\mathrm{Re}\int_0^\infty dt \exp\left[-\frac{\{t\Delta(T)\}^2}{4} - \right.$$
$$\left. t\{i(\bar\omega_{eg} + \lambda - \omega_{\mathrm{UV}}) + \tilde\Gamma_{eg}]G(t) \quad \text{(C1)}\right.$$

$$F(\omega_{\mathrm{UV}}) = 2\mathrm{Re}\int_0^\infty dt \exp\left[-\frac{\{t\Delta(T)\}^2}{4} - \right.$$
$$\left. t\{i(\bar\omega_{eg} - \lambda - \omega_{\mathrm{UV}}) + \tilde\Gamma_{eg}]G(-t) \quad \text{(C2)}\right.$$

where

$$\lambda = \sum_i^{N_{\mathrm{low}}} S_i\omega_i \quad \text{(C3a)}$$

Doubly Resonant IR−UV-vis Sum Frequency Generation

J. Phys. Chem. A, Vol. 106, No. 10, 2002 **2281**

$$\Delta^2(T) = \delta^2 + \delta^2(T) = \delta^2 + \sum_i^{N_{low}} 2S_i(1 + 2n_i)(\omega_i)^2 \quad \text{(C3b)}$$

and

$$G(t) = \exp[-\sum_j^{N_{high}} S_j\{1 - e^{-it\omega_j}\}] \quad \text{(C3c)}$$

From eqs C1 and C2, one can see that the so-called Stokes shift is given by 2λ and that using the results of $\Delta^2(T)$, $\bar{\omega}_{eg}$ and λ determined from the doubly resonant IR-vis SFG, we can reconstruct absorption and fluorescence spectra.

Appendix D: Nonresonant Terms

The second-order susceptibility can be given by[46]

$$\chi^{(2)}_{\alpha\beta\gamma}(\omega_I + \omega_{II}) = \chi^{(2)}_{\alpha\beta\gamma}(\omega_I + \omega_{II})_1 + \chi^{(2)}_{\alpha\beta\gamma}(\omega_I + \omega_{II})_2 + \\ \chi^{(2)}_{\alpha\beta\gamma}(\omega_I + \omega_{II})_3$$

where, for example,

$$\chi^{(2)}_{\alpha\beta\gamma}(\omega_I + \omega_{II})_1 = \frac{1}{\hbar^2}\sum_g\sum_m\sum_k\{\sigma_{gg}(T) - \sigma_{mm}(T)\}$$

$$\times \left[\mu_{gk}(\alpha)\left\{\frac{\mu_{mg}(\beta)\mu_{km}(\gamma)}{[(\omega_I - \omega_{mg}) + i\Gamma_{mg}][(\omega_I + \omega_{II} - \omega_{kg}) + i\Gamma_{kg}]}\right.\right. \quad \text{(D1)}$$

$$+ \frac{\mu_{mg}(\gamma)\mu_{km}(\beta)}{[(\omega_{II} - \omega_{mg}) + i\Gamma_{mg}][(\omega_I + \omega_{II} - \omega_{kg}) + i\Gamma_{kg}]}\bigg\} \quad \text{(D2)}$$

$$+ \mu_{kg}(\alpha)\left\{\frac{\mu_{mg}(\beta)\mu_{km}(\gamma)}{[-(\omega_I + \omega_{mg}) + i\Gamma_{mg}][(\omega_I + \omega_{II} + \omega_{kg}) + i\Gamma_{kg}]}\right. \quad \text{(D3)}$$

$$+ \frac{\mu_{mg}(\gamma)\mu_{km}(\beta)}{[-(\omega_{II} + \omega_{mg}) + i\Gamma_{mg}][-(\omega_I + \omega_{II} + \omega_{kg}) + i\Gamma_{kg}]}\bigg\}^* \quad \text{(D4)}$$

$$- \mu_{mk}(\alpha)\left\{\frac{\mu_{gm}(\beta)\mu_{kg}(\gamma)}{[(\omega_I - \omega_{gm}) + i\Gamma_{mg}][(\omega_I + \omega_{II} - \omega_{km}) + i\Gamma_{km}]}\right. \quad \text{(D5)}$$

$$+ \frac{\mu_{gm}(\gamma)\mu_{kg}(\beta)}{[(\omega_{II} - \omega_{gm}) + i\Gamma_{mg}][(\omega_I + \omega_{II} - \omega_{km}) + i\Gamma_{km}]}\bigg\} \quad \text{(D6)}$$

$$+ \mu_{km}(\alpha)$$

$$\left\{\frac{\mu_{gm}(\beta)\mu_{kg}(\gamma)}{[-(\omega_I + \omega_{gm}) + i\Gamma_{mg}][-(\omega_I + \omega_{II} + \omega_{km}) + i\Gamma_{km}]}\right. \quad \text{(D7)}$$

$$+ \frac{\mu_{gm}(\gamma)\mu_{kg}(\beta)}{[-(\omega_{II} + \omega_{gm}) + i\Gamma_{mg}][-(\omega_I + \omega_{II} + \omega_{km}) + i\Gamma_{km}]}\bigg\}^*\bigg] \quad \text{(D8)}$$

$\chi^{(2)}_{\alpha\beta\gamma}(\omega_I + \omega_{II})_2$ and $\chi^{(2)}_{\alpha\beta\gamma}(\omega_I + \omega_{II})_3$ can be obtained by $k \rightarrow m$ and $m \rightarrow k$, and $g \rightarrow k$ and $k \rightarrow g$ in eqs D1−D8, respectively.

Equation D1 is associated with the doubly resonant case, eqs D2 and D7 correspond to resonance−nonresonance mixing cases, and eqs D3, D4, D5, D6, and D8 are doubly nonresonant cases. Let us consider ratios of the intensities at specific doubly resonant frequencies where $\omega_I - \omega_{mg} = 0$ and $\omega_{II} - \omega_{km} = 0$.

Intensity ratios of eqs D2 and D7 to eq D1 can be approximately given by Γ_{mg}/ω_{II} and Γ_{mg}/ω_I, respectively. Or applying the B−O adiabatic approximation, these two ratios can be given by $\bar{\Gamma}_{gl}/\omega_{II}$ and $\bar{\Gamma}_{gl}/\omega_I$. Thus if only the doubly resonant case is considered, contributions of these two cases to $\chi^{(2)}_{\alpha\beta\gamma}(\omega_I + \omega_{II})_1$ can be ignored with respect to the doubly resonant case (eq D1). It is obvious that doubly nonresonant cases can also be ignored in similar fashion.

References and Notes

(1) Brown, F.; Parks, R. E.; Sleeper, A. M. *Phys. Rev. Lett.* **1965**, 1029.
(2) Meech, S. R. In *Advances in Multiphoton Processes and Spectroscopy*; Lin, S. H., Villaeys, A. A., Fujimura, Y., Eds.; World Scientific: Singapore, 1993; Vol. 8, p 281.
(3) Heinz, T. F.; Chen, C. K.; Ricard, D.; Shen. Y. R. *Phys. Rev. Lett.* **1982**, *48*, 478.
(4) Nguyen, D. C.; Muenchausen, R. E.; Keller, R. E.; Nogar, N. S. *Opt. Commun.* **1986**, *60*, 11.
(5) Hunt, J. H.; Guyot-Sionnest, P.; Shen, Y. R. *Chem. Phys. Lett.* **1987**, *133*, 189.
(6) Harris, A. L.; Chidsey, C. E. D.; Levins, N. J.; Loiacono, D. N. *Chem. Phys. Lett.* **1989**, *141*, 350.
(7) Superfine, R.; Huang, J. Y.; Shen, Y. R. *Phys. Rev. Lett.* **1991**, *66*, 1066.
(8) Akamatsu, N.; Domen, K.; Hirose, C.; Onishi, T.; Shimiza, H.; Masutani, K. *Chem. Phys. Lett.* **1991**, *181*, 175.
(9) Akamatsu, N.; Domen, K.; Hirose, C. *J. Phys. Chem.* **1993**, *97*, 10070.
(10) Owrutsky, J. C.; Culver, J. P.; Li, M.; Kim, Y. R.; Sarisky, M. J.; Yaganeh, M. S.; Yodh, A. H.; Hochstrasser, R. M. *J. Chem. Phys.* **1992**, *97*, 4421.
(11) Miraglitta, J.; Polizzotti, R. S.; Rabinowitz, R.; Cameron, S. D.; Hall, R. B. *Chem. Phys.* **1990**, *143*, 123.
(12) Hatch, S. R.; Polizzotti, R. S.; Dougal, S.; Rabinowitz, P. *Chem. Phys. Lett.* **1992**, *196*, 97.
(13) Shen, Y. R. *Solid State Commun.* **1992**, *94*, 171.
(14) Shen, Y. R. *The Principle of Nonlinear Optics*; Wiley: New York, 1984.
(15) Shen, Y. R. In *Frontiers in Laser Spectroscopy*; Hänsch, T. W., Inguscio, M., Eds.; North-Holland: Amsterdam, 1994; p 139.
(16) Duma, P.; Weldon, M. K.; Chabal, Y. J.; Williams, G. P. *Surf. Rev. Lett.* **1999**, *6*, 225.
(17) Huang, J. Y.; Shen, Y. R. *Phys. Rev. A* **1994**, *49*, 3973.
(18) Hizhnyakov, V.; Tehver I. *Phys. Status Solidi* **1967**, *21*, 755.
(19) Tonks, L.; Page, J. B. *Chem. Phys. Lett.* **1979**, *66*, 449.
(20) Blazej, D. C.; Peticolas, W. L. *J. Chem. Phys.* **1980**, *72*, 3134.
(21) Hassing, S.; Mortensen, O. S. *J. Chem. Phys.* **1980**, *73*, 1078.
(22) Page, J. B.; Tonks, D. L. *J. Chem. Phys.* **1981**, *73*, 1078.
(23) Champion, P. M.; Albrecht, A. C. *Chem. Phys. Lett.* **1981**, *82*, 410.
(24) Tehver, I. J. *Opt. Commun.* **1981**, *38*, 279.
(25) Tonks, D. L.; Page, J. B. *J. Chem. Phys.* **1982**, *76*, 5820.
(26) Champion, P. M.; Albrecht, A. C. *Annu. Rev. Phys. Chem.* **1982**, *33*, 353.
(27) Chan, C. K.; Page, J. B. *J. Chem. Phys.* **1983**, *79*, 5234.
(28) Stallard, B. R.; Champion P. M.; Callis, P. R.; Albrecht A. C. *J. Chem. Phys.* **1983**, *78*, 712.
(29) Chan, C. K. *J. Chem. Phys.* **1984**, *81*, 1614.
(30) Brafman, O.; Chan, C. K.; Khodadoost, B.; Page, J. B.; Walker, C. T. *J. Chem. Phys.* **1984**, *80*, 5406.
(31) Stallard, B. R.; Callis, P. R.; Champion P. R.; Albrecht A. C. *J. Chem. Phys.* **1984**, *80*, 70.
(32) Schomacher, K. T.; Bangcharoenpaurpong, O.; Champion, P. M. *J. Chem. Phys.* **1984**, *80*, 4701.
(33) Page, J. B. *Cryst. Lattice Defects Amorph. Mater.* **1985**, *12*, 273.
(34) Lee, S. A.; Chan, C. K.; Page, J. B.; Walker, C. T. *J. Chem. Phys.* **1986**, *84*, 2497.
(35) Cable, J. R.; Albrecht, A. C. *J. Chem. Phys.* **1986**, 84, 1969.
(36) Patapoff, T. W.; Turpin, P.; Peticolas, W. L. *J. Chem. Phys.* **1986**, *90*, 2347.
(37) Lu, H. M.; Page. J. B. *J. Chem. Phys.* **1988**, *88*, 3508.
(38) Page, J. B. In *Light Scattering in Solids VI: Topics in Applied Physics*; Cardona, M., Guntherodt, G., Eds.; Springer-Verlag: New York, 1991; Vol. 68, p 17.
(39) Lu, H. M.; Page, J. B. *J. Chem. Phys.* **1989**, *90*, 5315.
(40) Page, J. B.; Tonks, D. L. *J. Chem. Phys.* **1981**, *75*, 5694.
(41) Fujimura, Y.; Lin, S. H. *J. Chem. Phys.* **1979** *70*, 247. Fujimura, Y.; Lin, S. H. *J. Chem. Phys.* **1979**, *71*, 3733.
(42) Tang, J.; Albrecht, A. C. In *Raman Spectroscopy*; Szymanski, H. A., Ed.; Plenum Press: New York, 1970; Vol. 2, p 33.

2282 *J. Phys. Chem. A, Vol. 106, No. 10, 2002*

Hayashi et al.

(43) Boyd, R. W. *Nonlinear Optics*; Academic Press: San Diego, 1992.

(44) Lin, S. H.; Hayashi, M.; Lin, C. H.; Yu, J.; Villlayes, A. A.; Wu, G. Y. C. *Mol. Phys.* **1995**, *84*, 453.

(45) Lin, S. H.; Villayes, A. A. *Phys. Rev. A* **1994**, *50*, 5134.

(46) Lin, S. H.; Hayashi, M.; Islampour, R.; Yu, J.; Yang, D. Y.; Wu, G. Y. C. *Physica B* **1996**, *222*, 191.

(47) Islampour, R.; Hayashi, M.; Lin, S. H. *Chem. Phys. Lett.* **1995**, *234*, 7.

(48) Yan, Y. J.; Mukamel, S. *J. Chem. Phys.* **1986**, *85*, 5908.

(49) Condon, E. O. *Rev. Mod. Phys.* **1937**, *9*, 432.

(50) Shank, C. V.; Ippen, E. P.; Teschke, O. *Chem. Phys. Lett.* **1977**, *45*, 291.

(51) Hildebrandt, P.; Stockburger, M. *J. Phys. Chem.* **1984**, *88*, 5935.

(52) Takayanagi, M.; Hamaguchi, H.; Tasumi, M. *Chem. Phys. Lett.* **1986**, *128*, 555.

(53) Lin, S. H.; Alden, R. G.; Islampour, R.; Ma, H.; Villaeys, A. A. *Density Matrix Method and Femtosecond Processes*; World Scientific: Singapore, 1991.